Biosensors and Bioelectronics 123 (2019) 108–113

Contents lists available at ScienceDirect

Biosensors and Bioelectronics

journal homepage: www.elsevier.com/locate/bios

Organic electrochromic timer for enzymatic skin patches

Hiroyuki Kai, Wataru Suda, Shotaro Yoshida, Matsuhiko Nishizawa*

Department of Finemechanics, Tohoku University, 6-6-1 Aramaki Aoba, Sendai 980-8579, Japan

ARTICLE INFO

Keywords:
Electrochromism
Biofuel cell
Skin patch
Transdermal drug delivery
Wound healing

ABSTRACT

A totally organic and disposable electrochromic timer integrated with an enzymatic electrode and powered by biofuel cells is developed. The cathode of the self-powered electrochromic timer consists of a composite electrochromic film of poly(3,4-ethylenedioxythiophene) (PEDOT) and polyurethane (PU), while the anode is made up of a fructose dehydrogenase (FDH) enzymatic electrode. The electrochromic changes over time (up to 100 min) can be displayed in the device, and the speed of color change can be controlled by changing the resistance between the anode and the cathode. Automatic activation of the timer after placement on a skin is achieved by integrating a porous microneedle array. The electrochromic timer would be used along with a skin patch as a time-lapse display of medical and cosmetic treatments.

1. Introduction

Recent progress in printed electronics has opened up new possibilities for personalized medicine and ubiquitous healthcare (Kuribara et al., 2012; Sekitani and Someya, 2010; Rogers et al., 2010; Kim et al., 2012; Gao et al., 2016; Hattori et al., 2014; Benight et al., 2013). The flexibility of the printed electronic devices allows it to be used as skin patches for sweat sensor, intracranial fluid sensor, and iontophoretic drug delivery system (Dang et al., 2018; Griffith et al., 2018; Lee et al., 2017; Bandodkar et al., 2017). While most of the skin patches proposed so far focus on sensing vital information (Imani et al., 2016; Rose et al., 2015), they can be equally valuable for electrically stimulated medical treatments. For instance, induction of ionic current flow at a skin wound is known to accelerate the healing process by increasing the electromigration of keratinocytes towards the wounded surface (Funk, 2015; Song et al., 2002). Likewise, induction of ionic currents through the skin helps facilitate drug delivery and wrinkle removal (Dixit et al., 2007).

The electrical patches for sensing and stimulation need external power to run. These power sources are usually heavy, rigid, non-disposable, and hazardous (Saluja et al., 2013; Vikelis et al., 2012; Power, 2007). As a result, there is need for a built-in power source that is patient-compliant and easy to use. Enzymatic biofuel cells (BFCs) show some promise; they utilize the electrocatalytic properties of enzymes to produce electricity from biochemicals in a physiological environment, i.e., ambient temperature and at approximately neutral pH (Miyake et al., 2011a, b; Barton et al., 2004; Cooney et al., 2008; Heller, 2004; Meredith and Minteer, 2012; Kwon et al., 2014; Luckarift et al., 2014). Utilizing these properties of BFCs, we have recently fabricated a completely organic and disposable skin patch with a built-in BFCs for accelerating wound healing (Kai et al., 2017b), and transdermal drug dosing with iontophoresis (Ogawa et al., 2015a). These self-powered medical patches composed of enzyme-modified carbon fabrics, conducting polymer-based internal resistors, and hydrogel films containing fructose as the biofuel. One of the major challenges of the organic skin patch is the ability to measure and show the duration of elapsed time after the application of the patch. For example, the drug dosage to the skin depends on the duration that a drug was supplied through the skin patch (Lee et al., 2017). Thus, a visual cue to indicate when to dispose the patches can be very useful for controlling the drug dose.

In the present study, we have developed an electrochromic timer that works in conjunction with the system of enzymatic current generation. Limited flexibility of the existing electrochromic display (Yan et al., 2014; Chen et al., 2014) makes them incompatible for integrating into skin patches. However, by using a composite film of poly(3,4-ethylenedioxythiophene) and polyurethane (PEDOT/PU) (Kai et al., 2017a, b) we were able to make a stretchable electrochromic display the color depth of which indicates the amount of charge generated by the enzymatic skin patch. The enzymatic reaction-driven display indicates the time that has elapsed since the application of the patch (Fig. 1a). The electrochromic timer is composed of the PEDOT/PU film, a carbon electrode modified with fructose dehydrogenase (FDH) (Miyake et al., 2011a, b, 2013; Ogawa et al., 2015a, b), and hydrogel containing fructose (Fig. 1b). Color change of the PEDOT/PU film occurs when a current is generated from a redox reaction. A time lapse is monitored by tracking gradual changes in color depth of the PEDOT/PU

* Corresponding author.
E-mail address: nishizawa@biomems.mech.tohoku.ac.jp (M. Nishizawa).

https://doi.org/10.1016/j.bios.2018.07.013

Available online 10 July 2018

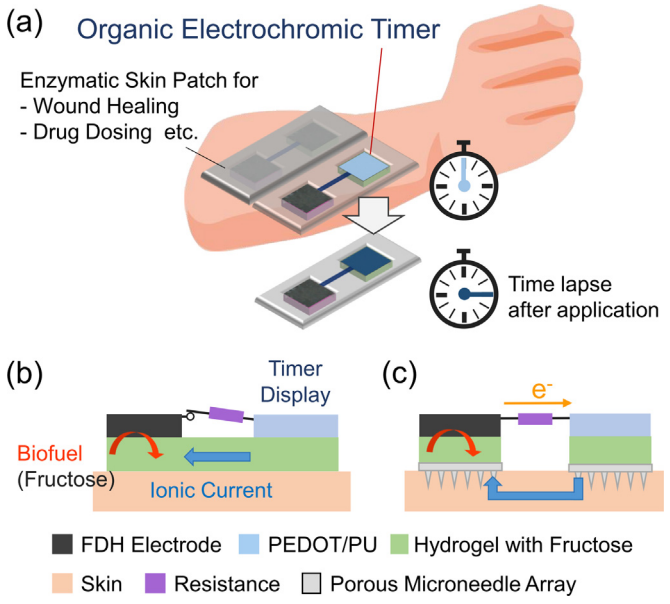

Fig. 1. Schematic of the organic electrochromic timer for enzymatic skin patches. (a) Concept of the electrochromic timer that displays a time lapse after application of a skin patch. (b) Structure of the electrochromic timer activated by closing an electric circuit with a resistance. (c) Structure of the electrochromic timer with an automatic activation switch after application to the skin.

film. The time lapse begins when the resistance and the FDH electrode are physically connected to the film. Further, the electrochromic timer is activated by interstitial fluid of the skin (Fig. 1c). Moreover, we show that the integration of a porous microneedle array (Liu et al., 2016; Nagamine et al., 2017) to the organic electrochromic timer is an effective way to achieve automatic activation (switch-on) of the timer immediately after applying it to the skin.

2. Experimental

2.1. Materials and equipment

Carbon nanotubes (CNTs; Baytube) were purchased from Bayer. Carbon fabric (TCC-3250) was purchased from Toho Tenax Co. Fructose dehydrogenase (FDH; FCD-302) was purchased from Toyobo. Polyurethane (PU; Gumthane AR650) was kindly provided by Okada Engineering. 3,4-Ethylenedioxythiophene (EDOT; Clevios MV2) and iron (III) tosylate ($Fe(III)(TsO)_3$; Clevios C-B 40 V2) were purchased from Heraeus. Polydimethylsiloxane (PDMS) pre-polymer and curing agent (Sylpot 184) were purchased from Dow Corning. Irgacure® 184 was purchased from BASF. Other reagents were purchased from Sigma Aldrich and Wako Pure Chemical, and were used as it is. All chemicals were used without further purification.

2.2. Preparation of a PEDOT/PU film

The composite film of poly(3,4-ethylenedioxythiophene) and polyurethane (PEDOT/PU) was prepared following the same procedure as in the previous study (Kai et al., 2017a, b). Briefly, glass slides (S1127, Matsunami Glass Ind., Ltd.) were cleaned by sonication in acetone, denatured ethanol, and distilled water three times; and then kept in isopropanol. PU was dissolved in tetrahydrofuran (THF) by stirring overnight at room temperature. EDOT, 1-butanol, and iron (III) tosylate were mixed to the THF solution and spin-coated on the glass slide at 2000 rpm for 30 s. The glass was heated to 90 °C on a hot plate to form PEDOT in the PU matrix. The resulting PEDOT/PU composite was washed in water on a shaker overnight to remove unreacted monomer and excess iron (III) tosylate. The fabricated PEDOT/PU film was subjected to electrochemical measurement as it was, or peeled off from the glass substrate to be used as a free-standing film. For measurement of color depth of the PEDOT/PU film in Figs. 2a, 1.667 ml of 10 wt% PU solution in THF, 0.799 ml of 1-butanol, 0.352 ml of EDOT, and 2.598 ml of 40 wt% iron(III) tosylate solution in 1-butanol were used. Otherwise, 5.000 ml of 10 wt% PU solution in THF, 0.286 ml of 1-butanol, 0.126 ml of EDOT, 0.929 ml of 40 wt% iron(III) tosylate solution in 1-butanol were used. Electric impedance of the fabricated PEDOT/PU electrode at high frequency was low (< 100 ohms/cm^2), and double-layer capacity of the PEDOT/PU electrode was 6.51 mF/cm^2.

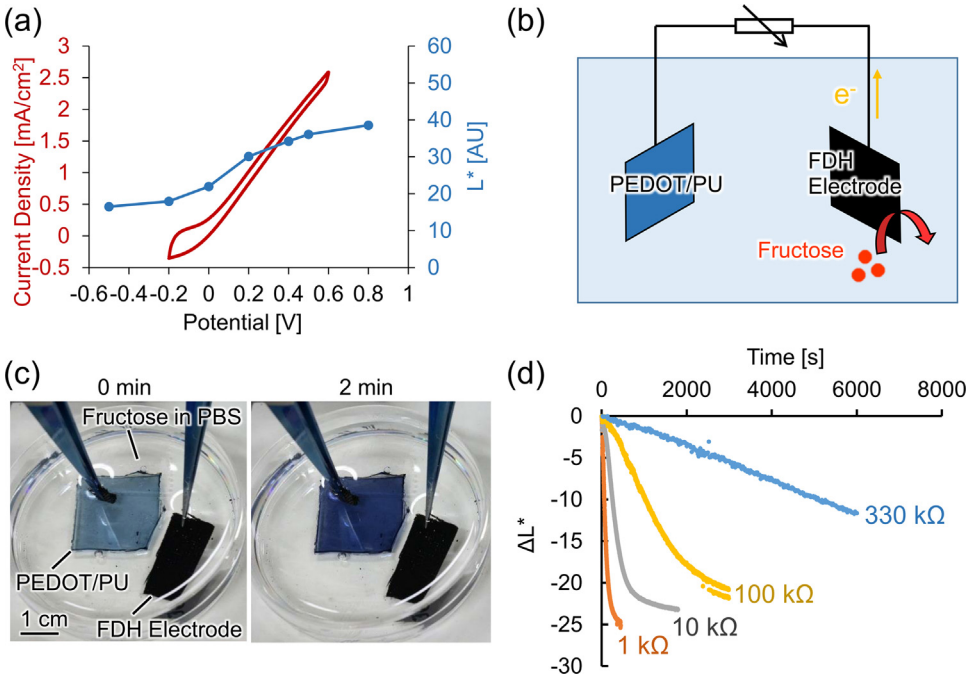

Fig. 2. Electrochromism of the PEDOT/PU film induced by FDH-catalyzed oxidation of fructose. (a) CV current of oxidation of fructose at an FDH electrode (red), and color depth of PEDOT/PU as a function of electrical potential (blue). (b) Schematic of measurement of color depth of a PEDOT/PU film connected to various resistances to a FDH electrode. (c) Color change of PEDOT/PU immersed in the fructose solution. (d) Time course of color change of PEDOT/PU with various resistances.

2.3. Preparation of an FDH electrode

The FDH-modified carbon fabric (CF) electrode was prepared according to the previous study (Miyake et al., 2011a, b). CNTs (40 mg) were heated to 400 °C in an oven for 11 h, then sonicated in a mixture of distilled water, sulfuric acid, and nitric acid (volume ratio 1:1:3) for 30 min. The CNTs in the solution were left at the room temperature for 5 h, neutralized by sodium hydroxide, and collected by filtration. The CNTs were frozen for 1 h, and dried in a freeze-dryer. The CNTs were sonicated in 1 wt% Triton-X aqueous solution (4 ml) by a tip sonicator to obtain the homogenous suspension. The suspension of CNTs (200 μl) was dropped on to a piece of carbon fabric (1 cm × 1 cm) and dried in an oven at 70 °C for 15 min. This was repeated 2 times on each side of the fabric. The carbon fabric was stirred in water for 1 h to remove excess CNTs and Triton-X. The fabric was immersed in a 50 mM McIlvaine buffer (pH 5.0) containing 5 mg/ml FDH and kept for more than 8 h at 4 °C.

2.4. Preparation of double-network hydrogel

A double-network hydrogel (DN hydrogel), composed of gellan gum crosslinked with Ca^{2+}, and poly(acrylamide) crosslinked with *N,N'*-methylenebis(acrylamide), was prepared as described in the previous study (Miyake et al., 2011a, b). Acrylamide (450 mg/ml), *N,N'*-methylenebis(acrylamide) (10 mg/ml), gellan gum (7.5 mg/ml), calcium chloride dihydrate (35.3 mg/ml), and Irgacure 184 (10 mg/ml) were mixed in water. The resulting mixture was heated in a microwave oven to the point of boiling, and poured between glass slides with a silicone rubber spacer of 0.5 mm thickness, followed by irradiation with 365 nm ultraviolet light for 1 h under nitrogen atmosphere. The polymerized hydrogel was washed in water on a shaker overnight, and further immersed in a 1X phosphate buffer saline (PBS) solution (pH 7) with or without 200 mM D-fructose on the shaker overnight.

2.5. Fabrication of a porous microneedle array

The porous microneedle array was prepared according to the previous report (Liu et al., 2016). The height and the diameter of each microneedle were 700 μm of 350 μm respectively. The array was composed of 6 × 6 conical needles with an interval of 1 mm. Briefly, a mold of the microneedle array was fabricated by drilling an acrylic plate, and molding it by PDMS (pre-polymer/curing agent with 10:1 w/w ratio, vacuum degassed for 1 h at room temperature). A mixture of 10 ml glycidyl methacrylate (GMA), 5.23 ml trimethylolpropane trimethacrylate (TRIM) and 15.7 ml triethylene glycol dimethacrylate (TEGDMA) was used as a monomer/cross-linker solution. 1 g of polyethylene glycol (PEG) in 5 ml of 2-methoxyethanol was used as a porogen that can be removed afterward. A mixture of 3 ml of the monomer/cross-linker solution, 3.5 ml of the porogen, and 9.7 mg of Irgacure 184 was poured onto the mold, and degassed in a vacuum chamber three times in 20 min to fill the mold with the solution. The mold was exposed to 365 nm ultraviolet light for 1 h to polymerize the mixture. After collecting the polymerized microneedle array from the mold, the porogen in the microneedle array was removed by immersing in ethanol/water (1:1 vol) at 50 °C for 4 h three times.

2.6. Electrochemical experiments

Electrochemical experiments were performed using a three-electrode system (BSA, 730C electrochemical analyzer) in stirred solutions at room temperature. The electrodes (PEDOT/PU film and FDH electrode) were mounted by SUS316L fine tweezers whose outer surface was insulated by resin, and electrically connected through a carbon resistor. Electrochemical potentials were reported as the voltage against Ag/AgCl in saturated KCl.

2.7. Evaluation of the color depth of a PEDOT/PU film

The movies of the electrochromic timer were taken by a digital camera (Canon EOS Kiss X7i), and RGB colors of every video frame were converted to the CIE L*a*b* color scale. L* values representing color depths were plotted against the time following the protocol used in our previous report (Kai et al., 2017a). Error bars indicated standard deviation between specimens.

3. Results and discussion

3.1. Electrochromism of PEDOT/PU driven by fructose oxidation at FDH electrodes

Fig. 2a shows the color depth of PEDOT/PU as a function of electrical potential (blue) and the CV current of oxidation of fructose at FDH electrode (red) at 10 mV/s, which were measured separately. Capacity of electric double layer of the FDH electrode was calculated from Fig. 2(a) as 9.64 mF/cm^2. The capacity charge of the wet electrode was relatively high compared to conventional dry metal electrodes. The PEDOT/PU composite film showed reversible electrochromism upon redox reactions as we previously reported (Kai et al., 2017a). The intrinsic conductivity of a PEDOT/PU composite eliminates the necessity of the underlying electrode for the color change of the entire film. The L* value of the PEDOT/PU film was a sigmoidal function of the applied voltage, and the midpoint of the sigmoidal shape that corresponded to the redox potential was around 0.1 V vs Ag/AgCl, which is in agreement with the previous findings (Kai et al., 2017a). The film under reduction reaction had a dark blue appearance when the supply voltage was below 0.1 V while the oxidized film appeared pale blue when voltage supply was above 0.1 V. On the other hand, the CV of the FDH-modified electrode showed that the oxidation of fructose started at − 0.2 V. The comparison of the reduction potential of PEDOT/PU (0.1 V) and the oxidation potential of fructose at FDH-modified electrode (− 0.2 V) indicated that the electrochromic color change of PEDOT/PU can be induced by FDH-catalyzed oxidation of fructose, in principle.

The PEDOT/PU film and an FDH-modified carbon fabric electrode were immersed in a 1 × PBS (pH7.0) containing 200 mM fructose, and externally connected as illustrated in Fig. 2b. Fig. 2c shows the system and the time lapse of the color change of the PEDOT/PU film in response to the addition of 200 mM fructose, where the external circuit was directly connected without a resistor. The color depth of the PEDOT/PU film was stable before the addition of fructose, and a sudden change to dark blue was observed within 2 min, indicating a smooth conjugation of the oxidation of fructose and the reduction of the PEDOT/PU film. The color depth of the PEDOT/PU film was stable even after addition of fructose when the external circuit was not connected. These results indicate that the direct reduction of PEDOT/PU by fructose is not possible (very slow), and the electrode catalyst, FDH in this case, is necessary for this conjugated redox system.

The enzymatic reaction-driven electrochromism of PEDOT/PU film was investigated by changing the external resistances (1, 10, 100, 330 kΩ) in 200 mM fructose in PBS. Fig. 2d shows the typical time courses of the variation of L* values from the initial (ΔL*) after the connection of a PEDOT/PU film and an FDH-modified electrode. The rate of color change of the PEDOT/PU film showed an inverse correlation with the resistance because the reaction speed of the system was controlled by the resistance value. Importantly, the change in speed for each resistance value was roughly constant, indicating the possible application of our system as the timer of which the range of measurement can be set using different resistance values.

3.2. Electrochromic timer in a skin patch format

To study the performance of the electrochromic timer in skin patch format, we integrated PEDOT/PU film and FDH-modified electrode on a

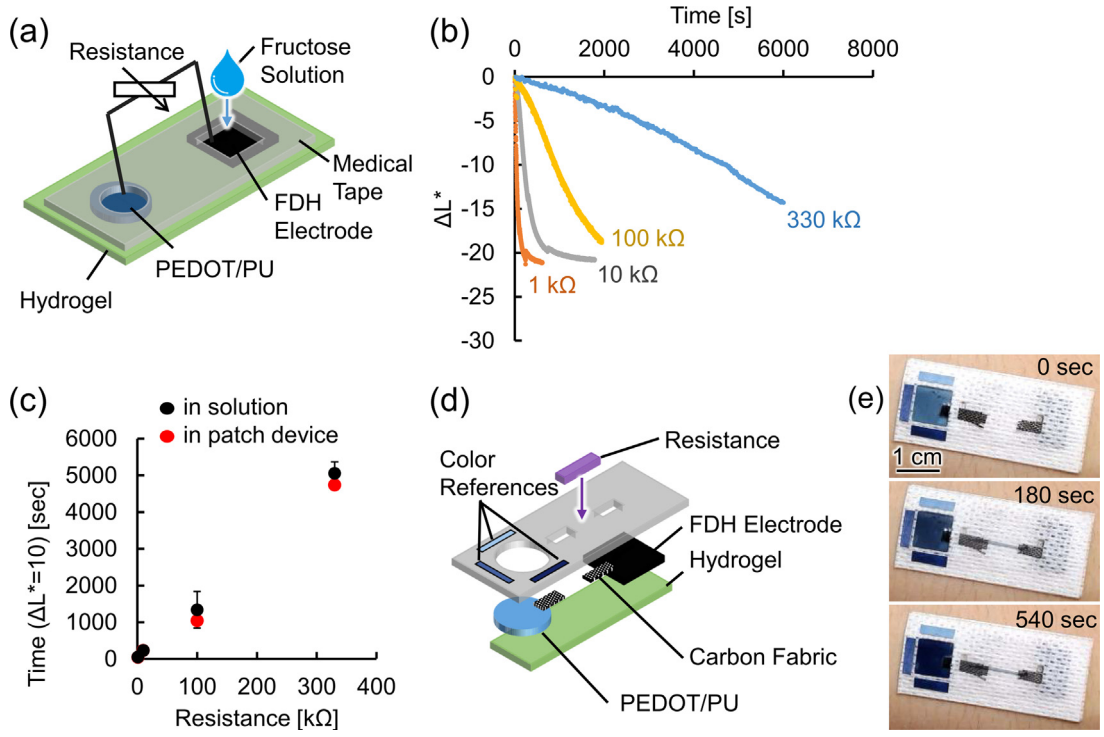

Fig. 3. The organic electrochromic timer in a skin patch format. (a) Schematic of the timer connected to various resistances, and activated by a drop of fructose solution. (b) Time course of color change of the PEDOT/PU in the skin patch. (c) Elapsed time for ΔL* = 10 as a function of connected resistances in bulk solution and in the form of a patch, respectively. (d) The totally organic electrochromic timer packed with internal biofuel in the hydrogel. (e) Time-lapse photographs of the timer after activation by connecting to a resistance.

piece of medical tape with two through holes for supplying fructose to the FDH-modified electrode and observing the PEDOT/PU film, respectively (Fig. 3a). The patch was placed on a DN hydrogel (0.5 mm thick) and various resistances (1, 10, 100, 330 kΩ) were connected. A droplet of 200 mM fructose in PBS was pipetted onto the FDH-modified electrode and ΔL* values of the PEDOT/PU film was monitored. Fig. 3b shows typical results obtained in the skin patch format, which were similar to the previous experiment in the stirred bulk solution (Fig. 2d). Especially, the color change in the early stage, the elapsed time for ΔL* = 10, was nearly identical (Fig. 3c). It is also shown here again that the range of measurable time can be set with the external resistance (n = 3 for each value of resistance).

Fig. 3d shows the structure of the totally organic enzymatic timer patch with a built-in power source. The electrochromic display of the PEDOT/PU film was exposed by a hole, while the FDH electrode was totally covered. A resistance made of PEDOT/PU film was externally placed on the device to connect PEDOT/PU film and the FDH electrode, and to set the range of the timer. In addition, to make the color change easily recognizable , the color references made of PEDOT/PU films with different degrees of oxidation (top: initial state, left: ΔL* = 10, bottom: reduced state) were adhered around the window of the display (Fig. 3e). The color of exposed PEDOT/PU timer was nearly the same as the top color reference at 0 s (before connection). As the electrochemical reaction proceeded after connecting to the resistance (10 kΩ), the color of the PEDOT/PU film changed, appeared to be the same as the left (ΔL* = 10) color reference at 180 s, and finally had the same color as the bottom (reduced state) color reference at 540 s. The relationship of the time and color change was in agreement with the results in Fig. 3c. With this setup, a user can roughly know the time even without any external complex equipment for the measurement of color. In addition, the change of L* values can be monitored in real-time by a mobile phone application (Kai et al., 2017a), therefore the time after skin patch application would be quantitatively measured using the organic, disposable electrochromic timer, benefiting on-site healthcare fields and cosmetic products. The FDH-modified electrode itself can be freeze-dried and stored for one week before use, however, when the FDH electrode is integrated in the patch device, it can be used for several hours (1–6 h) as far as we confirmed. The current configuration of the skin patch will be not suitable for long-term use but will be useful for one-day use disposable devices.

3.3. The timer with an automatic activation switch

The electrochromic timer in the skin patch format described above allowed measuring a time lapse after applying the fructose solution or an external resistance. Such mechanism of an activation switch (the application of fuel solution or the resistance) would be cumbersome for medical and cosmetic uses. For a more practical and smart switching mechanism of a timer, an electrochromic display integrated with a porous microneedle array was designed to directly activate the timer by closing the transdermal electric circuit when the patch is applied to the skin (Fig. 4a). A PEDOT/PU timer, a PEDOT/PU color reference, an FDH-modified electrode, two blocks of DN hydrogels, and a carbon electrode were packaged onto a medical tape with through holes and two PDMS sheets with holes. Two porous microneedle arrays were placed under the holes of the PDMS sheets. The PDMS sheets insulated the PEDOT/PU film and FDH-modified electrode such that they inhibited the on-skin ionic current (Nagamine et al., 2017). The porous microneedle array, which we reported previously (Liu et al., 2016), penetrates the stratum corneum of the skin and bypasses its high and variable resistance, resulting in a more controlled ionic current through the skin. The device was placed on the human skin, and the color change of the PEDOT/PU film was observed (Fig. 4b). The electrochromic timer showed nearly the same color as the color reference at 350 s after applying on the skin, as examined in the time course of L*, in which the color depth of the timer reached the value of the color reference after applying on the skin. On the other hand, the color depth of the timer placed on a piece of paper showed a constant value (black line

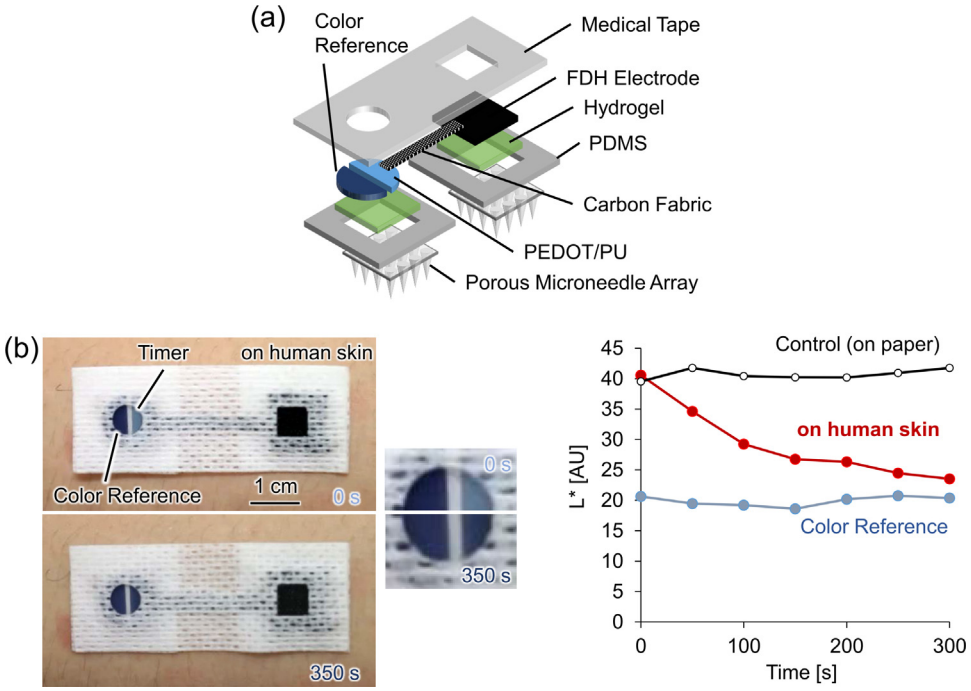

Fig. 4. The electrochromic timer integrated with porous microneedle arrays for automatic activation after applying on human skin. (a) Exploded view of the timer with porous microneedle arrays. (b) Left: Photographs of the timer after applying it on human skin immediately (top), and after 350 s (bottom), respectively. Inset shows the magnification of the timer. Right: Time courses of the color depth of the timer on human skin (red), a piece of paper (black), and the color reference (blue).

in the Fig. 4b). These results show that the integration of porous microneedle arrays to the electrochromic display helped realize the automatic activation switch of the timer.

4. Conclusions

In the present study, a totally organic and disposable electrochromic timer that can be used along with a skin patch was developed. This sensor is able to measure the time that elapsed since patching it to the skin. The comparison of the reduction potential of PEDOT/PU film and the oxidation potential of fructose at FDH electrode demonstrated that the electrochromic color change of the PEDOT/PU film can be induced by FDH-catalyzed oxidation of fructose. The starting time and the range of measurement of the timer can be modulated by a resistance connected between the PEDOT/PU film and the FDH electrode within a patch. A porous microneedle array integrated in the timer allowed automatic activation of the timer by closing the transdermal electric circuit when the patch is applied to the skin. The stability of the FDH electrode in a skin patch format was limited within one day, thus the electrochromic timer should be suitable for a disposable device. The electrochromic timer fabricated in this study looks promising for applications in healthcare/medical fields and cosmetics. Our future works will include integration of the electrochromic timer with drug dosing or wound healing skin patches to prove the device can be a versatile platform for displaying end time of the disposable skin patches.

Acknowledgements

The experiment that involved the application of a microneedle array to human skin was conducted according to the protocol approved by Tohoku University. This work was partly supported by MIRAI and Center of Innovation Program (COI-Stream) from Japan Science and Technology Agency (JST) and Grand-in-Aid for Scientific Research A (25246016) from the Ministry of Education, Culture, Sports, Science and Technology, Japan.

References

Kuribara, K., Wang, H., Uchiyama, N., Fukuda, K., Yokota, T., Zschieschang, U., Jaye, C., Fischer, D., Klauk, H., Yamamoto, T., Takimiya, K., Ikeda, M., Kuwabara, H., Sekitani, T., Loo, Y.L., Someya, T., 2012. Organic transistors with high thermal stability for medical applications. Nat. Commun. 3, 723–727. https://doi.org/10.1038/ncomms1721.

Bandodkar, A.J., You, J.-M., Kim, N.-H., Gu, Y., Kumar, R., Mohan, A.M.V., Kurniawan, J., Imani, S., Nakagawa, T., Parish, B., Parthasarathy, M., Mercier, P.P., Xu, S., Wang, J., 2017. Soft, stretchable, high power density electronic skin-based biofuel cells for scavenging energy from human sweat. Energy Environ. Sci. 10, 1581–1589. https://doi.org/10.1039/C7EE00865A.

Barton, S.C., Gallaway, J., Atanassov, P., 2004. Enzymatic biofuel cells for implantable and microscale devices. Chem. Rev. 104, 4867–4886. https://doi.org/10.1021/cr020719k.

Benight, S.J., Wang, C., Tok, J.B.H., Bao, Z., 2013. Stretchable and self-healing polymers and devices for electronic skin. Prog. Polym. Sci. 38, 1961–1977. https://doi.org/10.1016/j.progpolymsci.2013.08.001.

Chen, X., Lin, H., Deng, J., Zhang, Y., Sun, X., Chen, P., Fang, X., Zhang, Z., Guan, G., Peng, H., 2014. Electrochromic fiber-shaped supercapacitors. Adv. Mater. 26, 8126–8132. https://doi.org/10.1002/adma.201403243.

Cooney, M.J., Svoboda, V., Lau, C., Martin, G., Minteer, S.D., 2008. Enzyme catalysed biofuel cells. Energy Environ. Sci. 1, 320. https://doi.org/10.1039/b809009b.

Dang, W., Manjakkal, L., Navaraj, W.T., Lorenzelli, L., Vinciguerra, V., Dahiya, R., 2018. Stretchable wireless system for sweat pH monitoring. Biosens. Bioelectron. 107, 192–202. https://doi.org/10.1016/j.bios.2018.02.025.

Dixit, N., Bali, V., Baboota, S., Ahuja, A., Ali, J., 2007. Iontophoresis - an approach for controlled drug delivery: a review. Curr. Drug Deliv. 4, 1–10. https://doi.org/10.2174/156720107779314802.

Funk, R.H.W., 2015. Endogenous electric fields as guiding cue for cell migration. Front. Physiol. 6, 1–8. https://doi.org/10.3389/fphys.2015.00143.

Gao, W., Emaminejad, S., Nyein, H.Y.Y., Challa, S., Chen, K., Peck, A., Fahad, H.M., Ota, H., Shiraki, H., Kiriya, D., Lien, D.H., Brooks, G.A., Davis, R.W., Javey, A., 2016. Fully integrated wearable sensor arrays for multiplexed in situ perspiration analysis. Nature 529, 509–514. https://doi.org/10.1038/nature16521.

Griffith, J., Cluff, K., Eckerman, B., Aldrich, J., Becker, R., Moore-Jansen, P., Patterson, J., 2018. Non-Invasive Electromagnetic Skin Patch SensorNon-invasive electromagnetic skin patch sensor to Measure Intracranial Fluid–Volume Shiftsmeasure intracranial fluid–volume shifts. Sensors 18, 1022. https://doi.org/10.3390/s18041022.

Hattori, Y., Falgout, L., Lee, W., Jung, S.Y., Poon, E., Lee, J.W., Na, I., Geisler, A., Sadhwani, D., Zhang, Y., Su, Y., Wang, X., Liu, Z., Xia, J., Cheng, H., Webb, R.C., Bonifas, A.P., Won, P., Jeong, J.W., Jang, K.I., Song, Y.M., Nardone, B., Nodzenski, M., Fan, J.A., Huang, Y., West, D.P., Paller, A.S., Alam, M., Yeo, W.H., Rogers, J.A., 2014. Multifunctional skin-like electronics for quantitative, clinical monitoring of cutaneous wound healing. Adv. Healthc. Mater. 3, 1597–1607. https://doi.org/10.1002/adhm.201400073.

Heller, A., 2004. Miniature biofuel cells. Phys. Chem. Chem. Phys. 6, 209–216. https://doi.org/10.1039/B313149A.

Imani, S., Bandodkar, A.J., Mohan, A.M.V., Kumar, R., Yu, S., Wang, J., Mercier, P.P., 2016. A wearable chemical-electrophysiological hybrid biosensing system for real-time health and fitness monitoring. Nat. Commun. 7, 1–7. https://doi.org/10.1038/ncomms11650.

Kai, H., Suda, W., Ogawa, Y., Nagamine, K., Nishizawa, M., 2017a. Intrinsically stretchable electrochromic display by a composite film of poly(3,4-ethylenedioxythiophene)

and polyurethane. ACS Appl. Mater. Interfaces 9, 19513–19518. https://doi.org/10.1021/acsami.7b03124.
Kai, H., Yamauchi, T., Ogawa, Y., Tsubota, A., Magome, T., Miyake, T., Yamasaki, K., Nishizawa, M., 2017b. Accelerated wound healing on skin by electrical stimulation with a bioelectric plaster. Adv. Healthc. Mater. 6, 1–5. https://doi.org/10.1002/adhm.201700465.
Kim, D.-H., Ghaffari, R., Lu, N., Rogers, J.A., 2012. Flexible and stretchable electronics for biointegrated devices. Annu. Rev. Biomed. Eng. 14, 113–128. https://doi.org/10.1146/annurev-bioeng-071811-150018.
Kwon, C.H., Lee, S., Choi, Y., Lee, J.A., Kim, S.H., Spinks, G.M., Wallace, G.G., Lima, M.D., Kozlov, M.E., Baughman, R.H., Kim, S.J., 2014. High-power biofuel cell textiles from woven biscrolled carbon nanotube yarns. Nat. Commun. 5. https://doi.org/10.1038/ncomms4928.
Lee, J., Kwon, K., Kim, M., Min, J., Hwang, N.S., Kim, W.S., 2017. Transdermal iontophoresis patch with reverse electrodialysis. Drug Deliv. 24, 701–706. https://doi.org/10.1080/10717544.2017.1282555.
Liu, L., Kai, H., Nagamine, K., Ogawa, Y., Nishizawa, M., 2016. Porous polymer microneedles with interconnecting microchannels for rapid fluid transport. RSC Adv. 6, 48630–48635. https://doi.org/10.1039/C6RA07882F.
Luckarift, H.R., Atanassov, P.B., Johnson, G.R., 2014. Enzymatic Fuel Cells: From Fundamentals to Applications, First eded. John Wiley & Sons, New Jersey.
Meredith, M.T., Minteer, S.D., 2012. Biofuel cells: enhanced enzymatic bioelectrocatalysis. Annu Rev Anal Chem 5, 157–179. https://doi.org/10.1146/annurev-anchem-062011-143049.
Miyake, T., Haneda, K., Nagai, N., Yatagawa, Y., Onami, H., Yoshino, S., Abe, T., Nishizawa, M., 2011a. Enzymatic biofuel cells designed for direct power generation from biofluids in living organisms. Energy Environ. Sci. 4, 5008. https://doi.org/10.1039/c1ee02200h.
Miyake, T., Yoshino, S., Yamada, T., Hata, K., Nishizawa, M., 2011b. Self-regulating enzyme-nanotube ensemble films and their application as flexible electrodes for biofuel cells. J. Am. Chem. Soc. 133, 5129–5134. https://doi.org/10.1021/ja111517e.
Miyake, T., Haneda, K., Yoshino, S., Nishizawa, M., 2013. Flexible, layered biofuel cells. Biosens. Bioelectron. 40, 45–49. https://doi.org/10.1016/j.bios.2012.05.041.
Nagamine, K., Kubota, J., Kai, H., Ono, Y., Nishizawa, M., 2017. An array of porous microneedles for transdermal monitoring of intercellular swelling. Biomed. Micro. 19, 1–6. https://doi.org/10.1007/s10544-017-0207-y.
Ogawa, Y., Kato, K., Miyake, T., Nagamine, K., Ofuji, T., Yoshino, S., Nishizawa, M., 2015a. Organic transdermal iontophoresis patch with built-in biofuel cell. Adv. Healthc. MaterMater. 4, 506–510. https://doi.org/10.1002/adhm.201400457.
Ogawa, Y., Takai, Y., Kato, Y., Kai, H., Miyake, T., Nishizawa, M., 2015b. Stretchable biofuel cell with enzyme-modified conductive textiles. Biosens. Bioelectron. 74, 947–952. https://doi.org/10.1016/j.bios.2015.07.063.
Power, I., 2007. Fentanyl HCl iontophoretic transdermal system (ITS): clinical application of iontophoretic technology in the management of acute postoperative pain. Br. J. Anaesth. 98, 4–11. https://doi.org/10.1093/bja/ael314.
Rogers, J.A., Someya, T., Huang, Y., 2010. (review)MaterialsMaterials and Mechanicsmechanics for Stretchable Electronicsstretchable electronics. Science 327 (5973), 1603–1607. https://doi.org/10.1126/science.1182383.
Rose, D.P., Ratterman, M.E., Griffin, D.K., Hou, L., Kelley-Loughnane, N., Naik, R.R., Hagen, J.A., Papautsky, I., Heikenfeld, J.C., 2015. Adhesive RFID sensor patch for monitoring of sweat electrolytes. IEEE Trans. Biomed. Eng. 62, 1457–1465. https://doi.org/10.1109/TBME.2014.2369991.
Saluja, S., Kasha, P.C., Paturi, J., Anderson, C., Morris, R., Banga, A.K., 2013. A novel electronic skin patch for delivery and pharmacokinetic evaluation of donepezil following transdermal iontophoresis. Int. J. Pharm. 453, 395–399. https://doi.org/10.1016/j.ijpharm.2013.05.029.
Sekitani, T., Someya, T., 2010. Stretchable, large-area organic electronics. Adv. Mater. 22, 2228–2246. https://doi.org/10.1002/adma.200904054.
Song, B., Zhao, M., Forrester, J.V., McCaig, C.D., 2002. Electrical cues regulate the orientation and frequency of cell division and the rate of wound healing in vivo. Proc. Natl. Acad. Sci. USA 99, 13577–13582. https://doi.org/10.1073/pnas.202235299.
Vikelis, M., Mitsikostas, D.D., Rapoport, A.M., 2012. Sumatriptan transdermal iontophoretic patch (NP101-ZelrixTM): review of pharmacology, clinical efficacy, and safety in the acute treatment of migraine. Neuropsychiatr. Dis. Treat. 8, 429–434. https://doi.org/10.2147/NDT.S27456.
Yan, C., Kang, W., Wang, J., Cui, M., Wang, X., Foo, C.Y., Chee, K.J., Lee, P.S., 2014. Stretchable and wearable electrochromic devices. ACS Nano 8, 316–322. https://doi.org/10.1021/nn404061g.